Cellulose (2021) 28:2021–2038
https://doi.org/10.1007/s10570-020-03661-1

ORIGINAL RESEARCH

Conversion of low-quality cotton to bioplastics

Shaida S. Rumi · Sumedha Liyanage · Noureddine Abidi

Received: 28 October 2020 / Accepted: 24 December 2020 / Published online: 15 January 2021

Abstract The use of eco-friendly bioplastics has become a viable solution to reduce the accumulation of petrochemical products in the biosphere and to decrease microplastic contamination. In this study, we used low-quality cotton fibers that lack textile applications to prepare bioplastics. We dissolved cotton fibers in *N*,*N*-dimethylacetamide/lithium chloride (DMAc/LiCl) solvent system and converted cellulose solutions to strong, transparent, and flexible films through casting, gelation, regeneration, plasticization, and hot-pressing. Films were characterized using different analytical techniques to evaluate their physicochemical and mechanical properties. Compared to raw cotton cellulose, regenerated and hot-pressed cellulose films showed amorphous structures and excellent tensile characteristics. The physical and mechanical properties of cellulose films, such as deformation recovery, flexibility, homogeneity, elongation, and surface roughness, were significantly improved by means of plasticization and hot-pressing. Because glycerol plasticization increased the surface hydrophilicity of the films, plasma-induced surface grafting of oleic acid imparted hydrophobicity to cellulose films. This study presents a new avenue for using low-quality cotton fibers that are usually sold at a discounted price to produce value-added bioproducts for different applications.

Supplementary information The online version of this article (https://doi.org/10.1007/s10570-020-03661-1) contains supplementary material, which is available to authorized users.

S. S. Rumi · S. Liyanage · N. Abidi (✉)
Department of Plant and Soil Science, Fiber and Biopolymer Research Institute, Texas Tech University, Lubbock, TX 79409, USA
e-mail: noureddine.abidi@ttu.edu

Graphic abstract

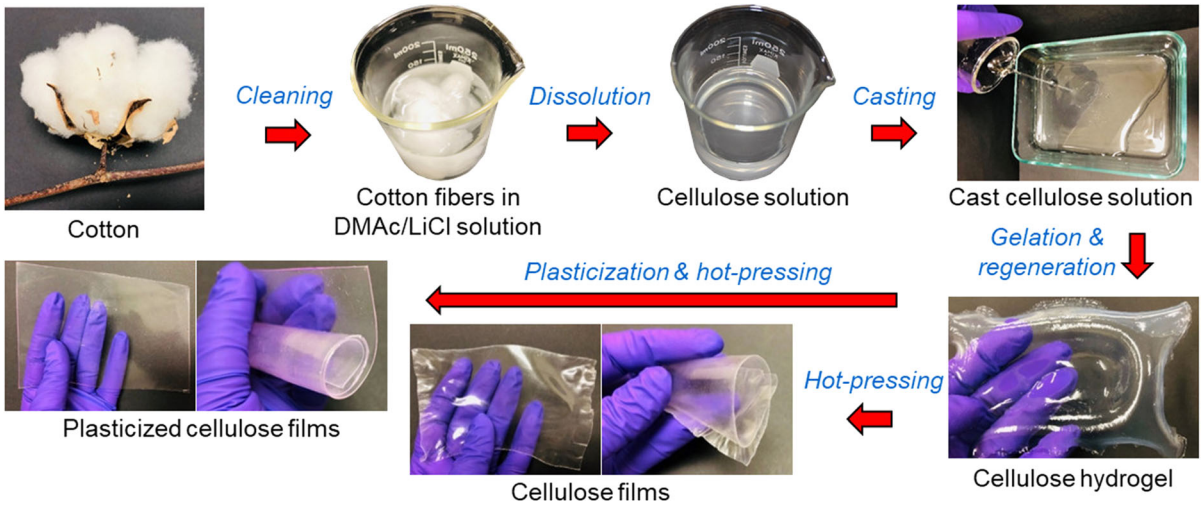

Keywords Cotton cellulose · Bioplastics · Plasticizer · Hot-pressing · Cellulose films

Introduction

The widespread use of plastic is creating a growing environmental concern. Every year, an extensive amount of plastic waste is generated and disposed of in the environment (Geyer et al. 2017). Global plastic pollution is occurring on a staggering scale, resulting in serious negative consequences (Laist 1997; Teuten et al. 2009; Tourinho et al. 2010; Law and Thompson 2014; Brennecke et al. 2015; Vethaak and Leslie 2016; Karami et al. 2017). While most unmanaged plastics end up in landfills and aquatic ecosystems, small broken pieces of plastic products (microplastics) are spreading throughout the biosphere at an alarming rate (Browne et al. 2011; Mathalon and Hill 2014; Ling et al. 2017). Microplastics easily wash through drainage systems and widely disperse in the air due to their light weight and end up in uninhabited rural ecosystems, animals, and even in human organs via food, water, and simply breathing. The production of bioplastics from nonfood agroforestry materials, such as wood and agricultural residues, is a possible alternative to petroleum-based plastics. However, effective conversion of biomass into bioplastics is challenging and requires purification and fractionation of the feedstock into its major components (e.g., cellulose, hemicelluloses, and lignin) (Brodin et al. 2017). As a result, the production of bioplastics from lignocellulosic biomass is considered demanding and not economically viable using the current production technologies (Brodin et al. 2017).

Cotton fibers are single elongated epidermal cells of cotton seeds (Abidi et al. 2010b) and are considered the purest form of plant cellulose in nature (Hsieh 2007). They contain approximately 95% cellulose after harvesting, ginning, and cleaning, whereas lignocellulosic biomass contains only 35–50% cellulose (Brodin et al. 2017). After scouring and bleaching, cotton fibers are composed of 99% cellulose. Cotton is a highly variable natural product, and its related fiber quality is often affected by several factors during the growing season. Specifically, undesirable extreme weather conditions during fiber development and maturation hinder cellulose synthesis and negatively impact molecular characteristics and cellulose organization in the secondary cell wall. Every year, a considerable amount of low-quality cotton, which is not qualified for traditional textile use, is harvested. Although low-grade cotton is sold at a discounted price, these fibers are a premium source of cellulose, which can be used to produce value-added materials for various applications. The high molecular weight of cotton cellulose translates into a remarkable mechanical strength of the final product. Moreover, this

process could create a new niche market for low-quality cotton.

Cellulose is a fascinating polymer with exceptional physiochemical and mechanical properties. It has a linear structure with anhydroglucose units (AGU) in thermodynamically preferred $^4C_1$ conformation (Klemm et al. 2005). Each AGU comprises three hydroxyl groups that establish numerous intra- and intermolecular hydrogen bonds between neighboring cellulose molecules, leading to a highly crystalline arrangement of cellulose fibrils along with less organized amorphous regions (Moon et al. 2011; Acharya et al. 2019). The rigidity of cellulose chains, the crystallinity, and the extensive intra- and intermolecular hydrogen bonds mainly contribute to its outstanding strength, chemical resilience, and other physical and mechanical properties (Hsieh 2007). As cellulose does not melt and decomposes when subjected to heat (Edgar et al. 2001), it is difficult to transform cellulose into desired forms. Consequently, dissolution is the predominant step in converting cotton fibers to new products. However, hydrogen bonds prevent cellulose dissolution in most common solvents, including organic solvents and water (Zhou and Zhang 2000). Therefore, it is important to select a solvent system that can effectively disrupt the extensive hydrogen bonding network within the fibers. The dissolution process of cotton cellulose is challenging compared to that of wood cellulose (a low crystallinity, a low degree of polymerization, and the presence of hemicellulose) because cotton fiber cellulose is characterized by high crystallinity and high molecular weight.

Nonderivatizing solvents are commonly used to break hydrogen bonds between cellulose chains (Sen et al. 2013). Such solvents include aqueous alkali solution, *N*-methylmorpholine-*N*-oxide (NMMO), *N*,*N*-dimethylacetamide/lithium chloride (DMAc/LiCl), and ionic liquids (McCormick et al. 1985; Fink et al. 2001; Zhang et al. 2001; Swatloski et al. 2002). Even though NaOH-based aqueous systems are environmentally friendly and economic, dissolution of cellulose having a high degree of polymerization ($DP > 300$) and a high molecular weight ($Mw > 1.2 \times 10^5$) is challenging (Qi et al. 2011; Luo and Zhang 2013). NMMO is used for direct dissolution of cellulose, but it is relatively expensive and causes unwanted harmful side reactions (Rosenau et al. 2002). Ionic liquids, commonly referred to as salts with melting points of approximately 100 °C (Rogers and Seddon 2003; Wang et al. 2012), have emerged as promising greener solvents to further diversify the applications of cellulose (Swatloski et al. 2002). They are considered sustainable alternatives to volatile organic solvents (Olivier-Bourbigou et al. 2010) and possess beneficial physiochemical properties. Ionic liquids have not created major environmental hazards, and nonflammability, high thermal stability, and high solvation ability are among their most beneficial physiochemical characteristics (Olivier-Bourbigou et al. 2010; Wang et al. 2012). However, their high processing viscosity, high cost, and hygroscopic nature limit their applications. DMAc/LiCl solvent system is a highly effective cellulose solvent that can dissolve highly crystalline and high-molecular weight cotton fibers under specific dissolution conditions. These conditions require minor adjustments depending on the molecular and crystallinity characteristics of cellulose. DMAc/LiCl solvent system is comparable with other solvents in terms of cost and recyclability (El Seoud et al. 2000), although its toxicity can cause environmental issues (Sayyed et al. 2019).

Several studies have reported on the effective conversion of low molecular weight cellulose, such as cotton linter pulp (Zhang et al. 2005; Lu et al. 2005; Wang et al. 2013), microcrystalline cellulose (MCC) (Acharya et al. 2017), wood pulp (Wang et al. 2013), and cellulose nanocrystals (CNCs) (Ma et al. 2011), to value-added products. The production of bioplastic films from cellulose derivatives (e.g., cellulose acetate) (Park et al. 2004) and cotton linters has also been reported (Zhang et al. 2001, 2002; Qi et al. 2011). Wang et al. reported the use of hot-pressing to convert cellulose pulp into bioplastic films (Wang et al. 2013). Herein, we prepared strong, flexible, and transparent films from low-quality cotton fibers through dissolution, regeneration, and hot-pressing. We further assessed their material characteristics, such as surface morphology, tensile properties, hydrophobicity/hydrophilicity, deformation recovery, thermal stability, and crystallinity.

Experimental

Materials

Extrapure DMAc (99%, A0403006) and anhydrous LiCl (99%, A0386841) were purchased from Acros Organics™ (NJ, USA). Glycerol (202397, certified ACS) and oleic acid (982133) were purchased from Fisher Scientific ™ (MA, USA). Low-quality cotton was collected from the Fiber and Biopolymer Research Institute (FBRI), Texas Tech University (Lubbock, TX, USA) and was scoured and beached following a general protocol reported in a previous study with a slight modification in caustic soda solution (concentration: 8%) (Abidi et al. 2007). The general scouring process uses 4% caustic soda, which could not completely clean low-quality cotton fibers with a high trash content. Therefore, the concentration of caustic soda was increased from 4 to 8% to remove the remaining trash content.

Sample preparation

Fiber dissolution

Scoured and bleached cotton fibers were dissolved in DMAc/LiCl solvent system using a protocol reported in a previous study with slight modifications (Acharya et al. 2017). First, oven-dried cotton fibers (105 °C, 24 h) were added to a hot DMAc solution at 80 °C (1% w:v) and stirred for 30 min. Next, oven-dried LiCl (8% w:v) was added into the solution, and stirring was continued for another 3 h at 80 °C. Then, the temperature was reduced to 50 °C, and the dissolution was continued overnight. Afterward, the solution was transferred to an oven (105 °C), and the progress of cotton fiber dissolution was evaluated using a polarized light microscope (Nikon Eclipse LV 100, Nikon Corporation, Tokyo, Japan) at different time points. After 12 h, the solution was removed from the oven and allowed to reach ambient temperature. At this stage, a clear cellulose solution was obtained, indicating complete cellulose dissolution. Solutions were always kept covered using aluminum foil during the dissolution process to prevent water adsorption.

Film preparation

Cellulose solution was cast into glass molds ($\sim$ 15 $\times$ 20 cm) and kept inside a fume hood for 24 h until a gel was formed. The gelated films were regenerated in deionized (DI) water for 5 days, and DI water was exchanged every 2 h. The regenerated cellulose films were plasticized with different concentrations of aqueous glycerol solutions (0, 10, 20, 30, 50, 75, and 99%) for 2 days. The plasticized films were hot-pressed at 120 °C for 15 min (Swing-Press20-0403, Across International, NJ, USA) (see supplementary materials- Fig. S1).

Hydrophobic functionalization

A microwave plasma treatment followed by oleic acid grafting was performed for hydrophobic functionalization (Cabrales and Abidi 2012). First, the hot-pressed cellulose films were subjected to microwave plasma treatment using Ar gas (flow rate = 60 mL/min, pressure = 25 Pa, generator frequency = 2.45 GHz, time = 240 s, power = 500 W). Plasma-activated films were immediately immersed in ethanol solutions containing different concentrations of oleic acid (0.066, 0.2, 0.3, 0.4, 0.6, 0.8, and 1.0 mol/L). Afterwards, the films were dried at room temperature and subjected again to plasma treatment for 240 s. Finally, the samples were rinsed with ethanol to remove nongrafted oleic acid and then dried under ambient conditions.

Material characterization

Cellulose films were conditioned in a controlled environment for 48 h (relative humidity of 65 $\pm$ 2% and temperature of 21 $\pm$ 1 °C) before characterization.

Scanning electron microscopy (SEM)

Scanning electron microscopy micrographs were collected from cellulose films to study the surface morphology of the films. Samples were mounted on an aluminum stub covered with carbon conductive tapes (Ted Pella Inc, Redding, CA, USA) and visualized using SEM (TM-1000, Hitachi, Japan) with an accelerating voltage of 15 kV.

Fourier transform infrared spectroscopy (FTIR)

FTIR spectra of cotton fibers and regenerated cellulose films were recorded using Spectrum 400 FTIR instrument (PerkinElmer, MA, USA) equipped with a ZnSe diamond crystal and a pressure arm. Three spectra were recorded from each sample (spectral resolution: 4 cm^{-1} and 32 coadded scans) in the mid-infrared (IR) range between 4000 and 650 cm^{-1}. Baseline correction and normalization were performed using Spectrum software (PerkinElmer, MA, USA). The IR crystallinity index (i.e., the integrated peak intensity ratio 1429/897 cm^{-1}) was also calculated using Spectrum software to study the changes in the crystalline domain of cellulose.

Thermogravimetric analysis (TGA)

The thermal properties of cotton fibers and regenerated cellulose films were analyzed using a Pyris 1 thermogravimetric analyzer (PerkinElmer, MA, USA). Cotton fibers and small pieces of cellulose films were placed in crucibles, and thermograms were recorded between 37 and 600 °C with a heating rate of 10 °C/min under a constant flow of nitrogen (20 ml/min). The percent weight loss, first derivatives of the thermograms, and peak decomposition temperatures of each sample were calculated using Pyris data analysis software (PerkinElmer, MA, USA).

X-ray diffraction (XRD)

X-ray diffraction patterns of samples were recorded at ambient temperature using a SmartLab X-ray diffractometer (HD 2711 N, Rigaku, Japan) equipped with nickel-filtered Cu-Kα radiation generated at 40 kV and 44 mA (λ = 0.154 nm). Samples were placed on the glass slide sample holder, and scans between 10° and 50° were performed with a scanning speed of 2°/min. The diffraction pattern of the sample holder was recorded first and subtracted from the diffraction patterns of the samples. Peak fitting was carried out using PeakFit software (v4.12, https://systatsoftware.com) assuming a Gaussian function for each peak ($R^2 > 90\%$). The crystallinity index was calculated using the following equation (Hu and Abidi 2016):

$$Crystallinity\ index(\%) = \frac{\sum area\ of\ crystalline\ peaks}{\sum area\ of\ crystalline\ and\ amorphous\ peaks} \times 100$$

Deformation recovery

The recovery of films from bending deformation was determined using a crease recovery tester (James H. Heal & Co. Ltd., Halifax, England) (see supplementary materials-Fig. S2). The AATCC 66-2008 test method was used to measure the recovery angle. The test specimen (40 × 15 mm) was folded and compressed using a 500 g force for 5 min. Next, the folded test specimen was clamped to the recovery angle measurement tester for a recovery period of 5 min, and the recovery angle was recorded. Three replications (films) were performed for each glycerol concentration, and six specimens were tested from each film.

Moisture absorption

The moisture absorption properties of cellulose films were determined according to ASTM D570 guideline. Cellulose films were dried at 105 °C until a constant weight was reached and consequently transferred to a desiccator. Once the samples reached ambient temperature, the weight was recorded (W_d: dry weight). Next, the weighed films were placed on a mesh that was placed on a petri dish filled with distilled water. The system was transferred to a controlled environment (65 ± 2% relative humidity and 21 ± 1 °C), and the weight of each film (W_m) was recorded at different time intervals (1, 2, 3, 4, 5, 6, 8, 12, 15, 18, and 24 h). Moisture absorption was calculated using the following equation:

$$\text{Increase in weight } (\%) = \frac{W_m - W_d}{W_d} \times 100$$

where W_m = weight of the film as a function of time and W_d = dry weight.

Dynamic contact angle

The efficiency of the surface grafting with oleic acid was evaluated using a drop shape instrument (FTA1000, First Ten Angstroms Inc, CA, USA). Water droplets (5 µL) were dispensed onto the surface

of the film using syringe assembly (30-gauge needle), and images were recorded every 3 s for 120 s. The dynamic contact angles of the air-liquid-solid interface were calculated using the software of the instrument (Cabrales and Abidi 2012).

Tensile testing

Test specimens were prepared according to ASTM D638-14 guidelines (ASTM-D638-14 2015). First, cellulose films were placed flat on the specimen stage of a manual clicker press (Qualitest, USA: https://www.worldoftest.com/). Then, an ASTM D638- Type IV tensile die was placed on the sample and pressed using the pressure arm of the clicker press. The thickness of the test specimens was measured at the center of the specimen according to ASTM D638-14 guidelines. The tensile properties of cellulose films were also recorded as per the ASTM 638-14 guidelines using the Multi-Test 2.5-dV(u) Test System (Mecmesin, UK). The griping distance and the speed of the instrument were set to 65 mm and 50 ± 10 mm/min, respectively. A large number of cellulose films prepared from four individual batches (individual replicates) and 4–5 films were prepared from each batch. Three to four specimens were prepared from each film, and 12–15 specimens were tested from each replicate.

Statistical analysis

One-way analysis of variance (ANOVA) was performed using STATISTICA (Version 13.3; July 2018; TIBCO software, CA, USA).

Results and discussion

Dissolution of cotton fiber in DMAc/LiCl solvent system

In this study, intact cotton fibers were dissolved using a protocol used to dissolve microcrystalline cellulose (Acharya et al. 2017). MCC is generally derived from wood. It has a low molecular weight and smaller particle size compared to cellulose derived from cotton fibers. As expected, this protocol did not successfully dissolve cotton fibers. At the end of 24 h, undissolved cotton fibers were still visible in the solution. Therefore, the dissolution was continued at 105 °C for an additional 12 h and was monitored using polarized light microscopy. Figure 1 shows polarized light microscopy images of 1% (w:v) cotton fibers in DMAc/LiCl solvent system at different times (0, 6, 9, and 12 h). According to these images, heating the solution at 105 °C improved fiber dissolution. After 12 h, only a few cotton fiber fragments were observed. Further heating at 105 °C led to discoloration of the solution.

Regeneration, plasticization, and hot pressing of cellulose films

Figure 2 shows the different steps followed during the conversion of cotton cellulose solution (1% w:v) into transparent and flexible films. After dissolution for an additional 12 h at 105 °C, the solution becomes viscous and clear (Fig. 2a). The regenerated cellulose hydrogel remains transparent and flexible (Fig. 2b). Glycerol plasticization does not cause drastic changes in hydrogels. However, plasticization with over 30% aqueous glycerol solution seems to affect the integrity of cellulose hydrogels. Cellulose hydrogels become increasingly fragile when the glycerol concentration exceeds 30%. Similarly, extending the plasticization period beyond 48 h also affects the integrity of hydrogels. These hydrogels tend to break during hot-pressing. The average thickness of cellulose hydrogels is approximately 2 mm. The physical and mechanical properties of dry cellulose films appear to be affected by plasticization and the drying technique. For example, cellulose hydrogels substantially shrink during air-drying and produce opaque, strong, nonflexible, and irregularly shaped materials (Fig. 2d).

Regenerated cellulose hydrogels also noticeably shrink during hot-pressing. The hot-pressed films show some degree of surface unevenness and stiffness but are transparent, smooth, and strong (Fig. 2e). Cellulose dissolution breaks hydrogen bonds that hold cellulose molecules together, and gelation and regeneration in deionized water allow hydrogen bonds to reform. As a result, cellulose chains aggregate and produce a hydrogel that often takes the shape of the mold that is used for casting the cellulose solution. Hot-pressing helps to stretch and rearrange cellulose chains and form a layered dense packing structure (Wang et al. 2013).

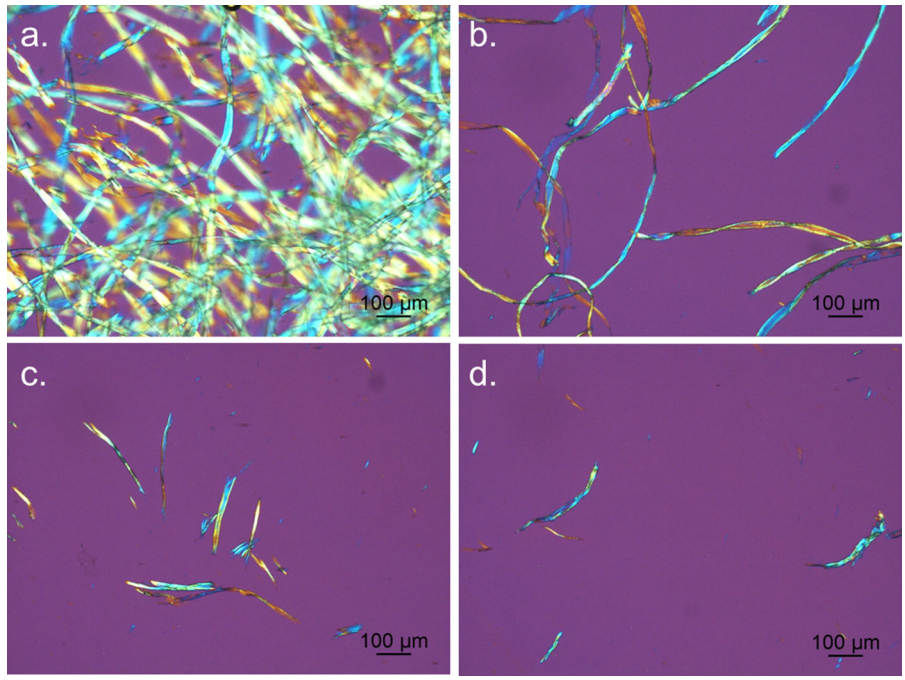

Fig. 1 Polarized light microscopy images of 1% cotton fibers (w:v) in a DMAc/LiCl solvent system at 105 °C (magnification—10 x). **a** Before transferring the solution to an oven at 105 °C and after **b** 6 h, **c** 9 h, and **d** 12 h at 105 °C

The use of a plasticizer improves the workability and flexibility of plastic films (Suyatma et al. 2005). The polymer–polymer interactions are reduced by the plasticizer; consequently, the rigidity or stiffness of the three-dimensional film structure is decreased. As a result, the plasticizer allows the deformation of bioplastics without rupture (Mekonnen et al. 2013). The plasticized and hot-pressed cellulose films exhibit improved flexibility and homogeneity compared to the properties of nonplasticized films (Fig. 2f). The plasticized and hot-pressed cellulose films are transparent and can be rolled without conspicuous breakage.

These results show that hot-pressing plays a key role during the transformation of cellulose hydrogel into a transparent, flexible, strong, and uniform film. Hot-pressing reduces surface roughness and produces smooth and homogeneous films. The average thickness of hot-pressed cellulose films is 0.2 ± 0.08 mm and that of plasticized cellulose films is 0.50 ± 0.07 mm ($n = 48$). The variability within each type of film could be attributed to inconsistencies introduced during hot pressing (i.e., pressure or gap between lower and upper plates of the hot press). SEM images show the surface morphology of hot-pressed cellulose films, and no major morphological differences are observed due to plasticization. Both types of hot-pressed films show smooth surface morphology with few defects/stress marks introduced during hot-pressing. Few fiber fragments are still present on the film surface.

FTIR characterization

Figure 3a shows the FTIR spectra acquired from cotton fibers and nonplasticized cellulose films. Dissolution of cotton fibers followed by regeneration created major changes in the FTIR spectra. The characteristic peaks of native cellulose at 3334 and 3293 cm^{-1}, assigned to OH stretching vibrations, provided information regarding the intra- and intermolecular hydrogen bonds (Carrillo et al. 2004; Abidi et al. 2010a). These OH stretching vibrations in the spectra of the regenerated cellulose film became broader and shifted to a higher wavenumber (3350 cm^{-1}). This suggested that the crystalline structure of cotton cellulose was disrupted during the dissolution process, and therefore, the regenerated samples have an abundance of free hydroxyl groups (Ciolacu et al. 2011; Lan et al. 2011). These changes were also accompanied by a pronounced increase in

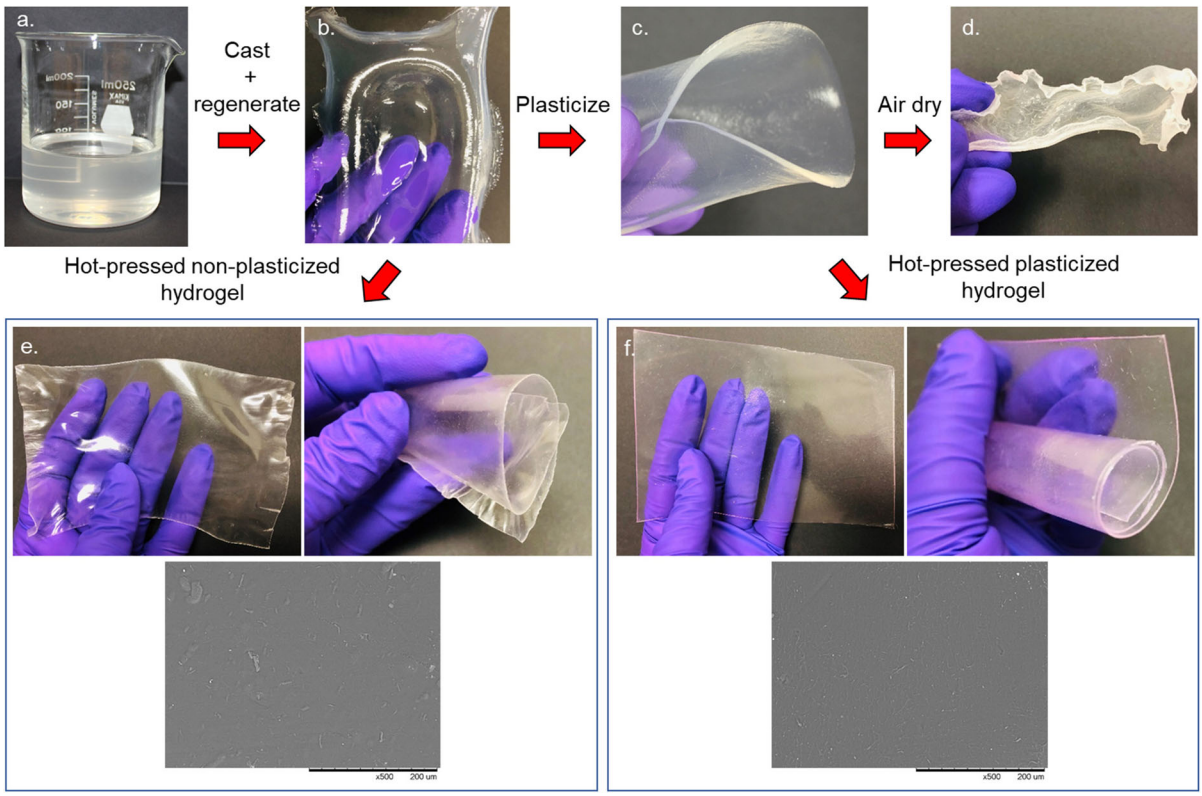

Fig. 2 Conversion of cellulose solution into flexible and transparent films. **a** Clear solution of 1% (w:v) cotton fibers dissolved in a DMAc/LiCl solvent, **b** cellulose hydrogel after gelation and regeneration in deionized water for 5 days, **c** cellulose hydrogel plasticized with glycerol, **d** air dried cellulose film, **e** visual images and an SEM micrograph (× 500) of hot-pressed cellulose films (nonplasticized) and **f** visual images and an SEM micrograph (× 500) of hot-pressed cellulose films (plasticized)

peak intensities at 1640 cm^{-1} and 897 cm^{-1}, which were attributed to O–H bending of adsorbed water and β-linkage of cellulose, respectively. This is because dissolution followed by regeneration increases the amorphous region of cellulose, which in turn facilitates water adsorption and accessibility of β-linkage by the IR beam (Ciolacu et al. 2011; Liyanage and Abidi 2019). Similar changes in the IR band at 897 cm^{-1} have been reported due to the regeneration of native cellulose (Ciolacu et al. 2011; Dissanayake et al. 2019). In addition, the vibration at 1427 cm^{-1} (CH_2 scissoring referred to as a crystalline absorption band of cellulose) became broad and shifted to 1439 cm^{-1} in the regenerated film, suggesting the destruction of intramolecular hydrogen bonds and the crystalline structures of cellulose (Nelson and Mares 1965; Zhou et al. 2002; Zhang et al. 2002). In addition, the IR vibrations of native cellulose located at 1314, 1108, 1054, and 985 cm^{-1}, originating from C–H bending, asymmetric ring stretching, C–O stretching, and ring stretching mode, respectively, were not visible in the spectra of regenerated cellulose films. The disappearance of the absorption bands of native cellulose suggests alterations of the crystalline structure of cellulose (Ciolacu et al. 2011).

Figure 3b shows the FTIR spectra of hot-pressed cellulose films prepared from nonplasticized and glycerol plasticized hydrogels. The plasticized cellulose films show major IR bands originating from glycerol (e.g., 2934, 2880, 1415, 1157, 1030, 993, 922, and 851 cm^{-1}). In addition, some IR vibrations (e.g., 1108 and 897 cm^{-1}) assigned to cellulose disappeared when glycerol was applied. The OH stretching vibrations at 3284 cm^{-1} became broad and intense in the plasticized cellulose films, implying that the intra- and intermolecular bonding of cellulose changed due to glycerol plasticization. The peak intensities of several IR bands seemed to change with increasing

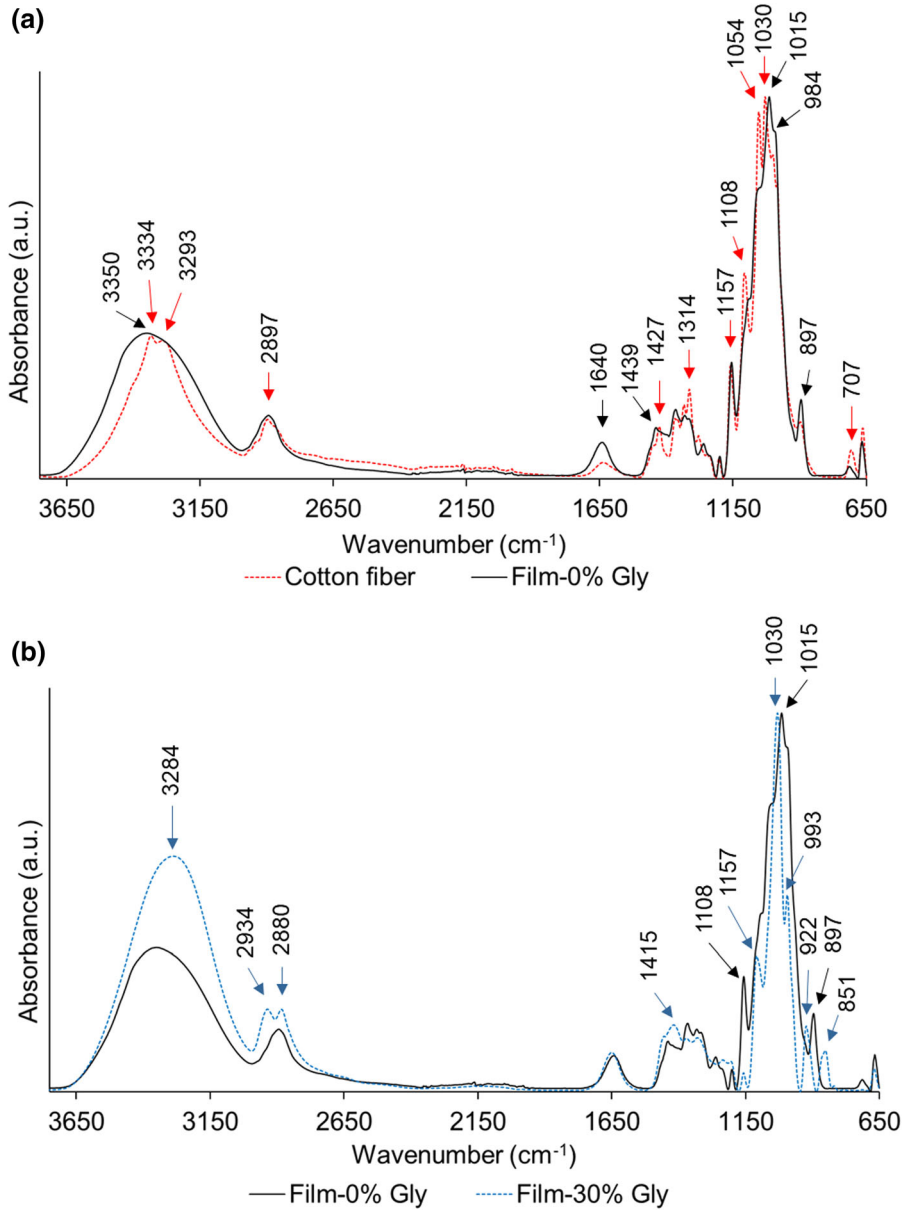

Fig. 3 FTIR spectra acquired from cotton fibers and nonplasticized (Film-0% Gly) and plasticized cellulose films (Film-30% Gly). **a** Comparison between FTIR spectra of cotton fibers and nonplasticized cellulose films and **b** a comparison between FTIR spectra of nonplasticized and plasticized cellulose films

concentrations of glycerol (see supplementary materials-Fig. S3).

As discussed above, the changes in the peak intensities of several characteristic IR vibrations indicated the disruption of the crystalline structure of cellulose (Zhang et al. 2002; Oh et al. 2005; Gwon et al. 2010; Ciolacu et al. 2011). The peak intensity ratio of 1429/897 cm^{-1} was termed the IR lateral order index (Hurtubise and Krassig 1960). It serves as empirical crystallinity index of cellulose (Abidi et al. 2014) and is positively correlated to the change in cellulose crystallinity (Liyanage and Abidi 2019). Due to dissolution and regeneration, the intensity of the vibration at 1429 cm^{-1} decreased, and the intensity of the vibration at 897 cm^{-1} increased. As a result, the IR

lateral order index was significantly reduced from 2.28 ± 0.35 to 0.48 ± 0.03 (n = 6 and $p \leq 0.05$).

X-ray characterization

Figure 4a shows the XRD patterns of cotton fibers and cellulose films plasticized with different concentrations of glycerol. The XRD pattern of cotton fiber showed typical diffraction peaks of cellulose I at 2θ = 14.7°, 16.5°, 22.7°, and 34.4° corresponding to crystal planes (hkl) of $1\bar{1}0$, 110, 200, and 004, respectively (French 2014). In X-ray diffractograms of regenerated cellulose films, sharp crystalline peaks at 2θ values of approximately 14.7°, 16.5°, and 22.7° were absent, and instead, a broad and weak crystalline peak was observed around the 200 (hkl) plane. The XRD patterns of these cellulose films appear identical to those of amorphous cellulose structures (Ciolacu et al. 2011). XRD data were smoothed using PDXL software (Rigaku, Japan) and exported to PeakFit

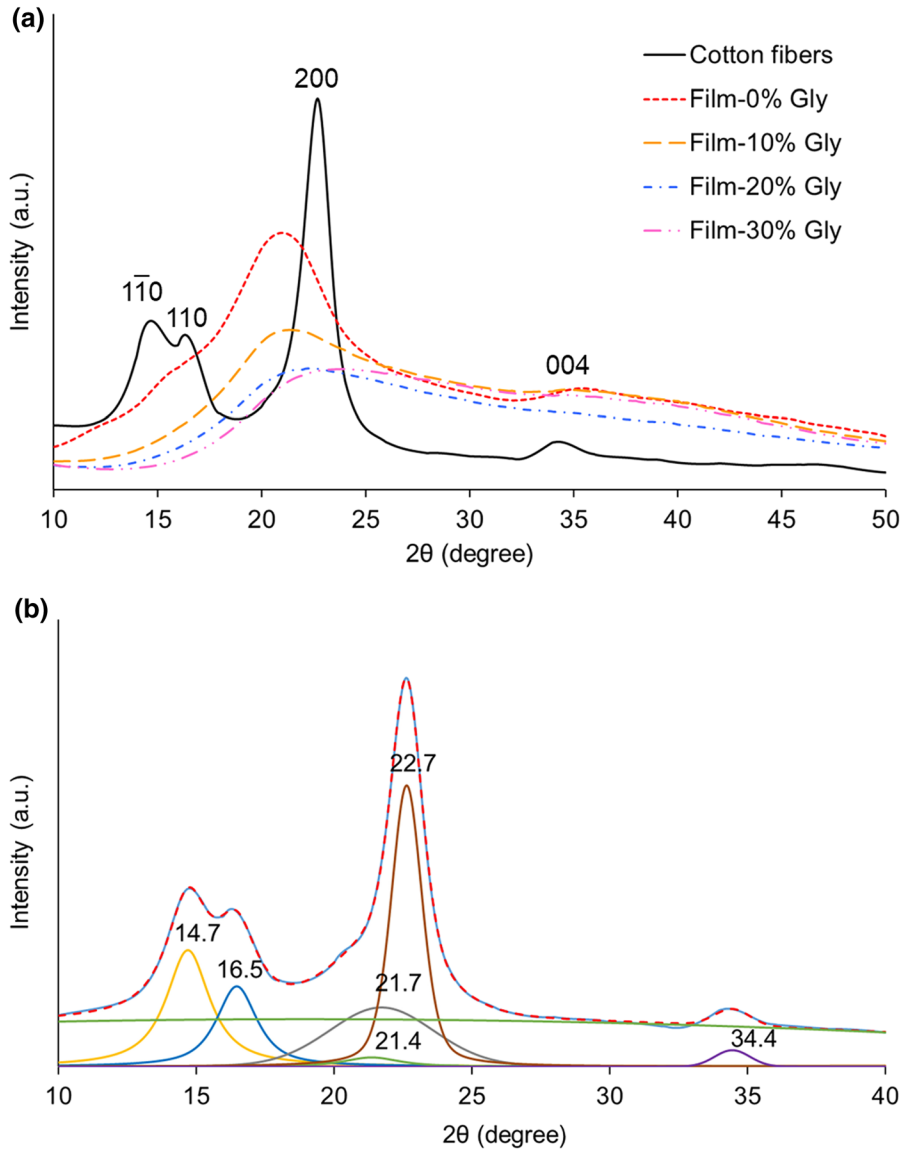

Fig. 4 X-ray diffraction analysis of samples. **a** X-ray diffractograms of cotton fibers and cellulose films plasticized with different concentrations of glycerol (0, 10, 20, and 30% glycerol) and **b** an example of peak fitting using PeakFit software

software; peak fitting was performed using Gaussian functions (Fig. 4b). Cotton fibers showed a 78% crystallinity index, and cellulose films showed much lower crystallinity indices that ranged between 32 and 42%. As expected, this change in crystallinity was attributed to the disruption of well-organized native cellulose microstructures followed by the development of more amorphous cellulose structures in bioplastic films. The presence of amorphous cellulose is highly advantageous for film flexibility and elongation. In addition, amorphous cellulose has more accessible OH groups that could serve as active sites for material functionalization to introduce new functionalities or to improve their mechanical properties.

TGA characterization

TGA thermograms and first derivative thermogravimetry of cotton fiber and cellulose films plasticized with different concentrations of glycerol are shown in Fig. 5. TGA thermograms of nonplasticized cellulose films were identical to those of cotton fibers and showed two main weight loss regions (37–100 °C and 250–450 °C). In addition to these two weight loss regions that were attributed to the removal of adsorbed water and decomposition of cellulose (Abidi et al. 2008; Acharya et al. 2017), the films treated with glycerol showed an additional weight loss region between 100 and 250 °C. The weight loss between 100 and 250 °C was attributed to the decomposition of glycerol (thermogram of glycerol is shown in supplementary materials—Fig. S4). Regenerated cellulose films showed significantly higher weight loss between 37 and 100 °C ($p \leq 0.05$) compared to cotton fibers (Fig. 5c). This is because cellulose films have more amorphous regions with free hydroxyl groups that can adsorb more water molecules though hydrogen bonding (Acharya et al. 2017). The effect of glycerol treatment on weight loss (%) was also significant, probably due to the hygroscopic nature of glycerol ($p \leq 0.05$). However, there was no significant effect of glycerol concentration on the adsorbed water content of cellulose films ($p \leq 0.05$).

The peak decomposition temperature of cotton fibers was observed at approximately 381 °C (Fig. 5d). All regenerated films showed significantly

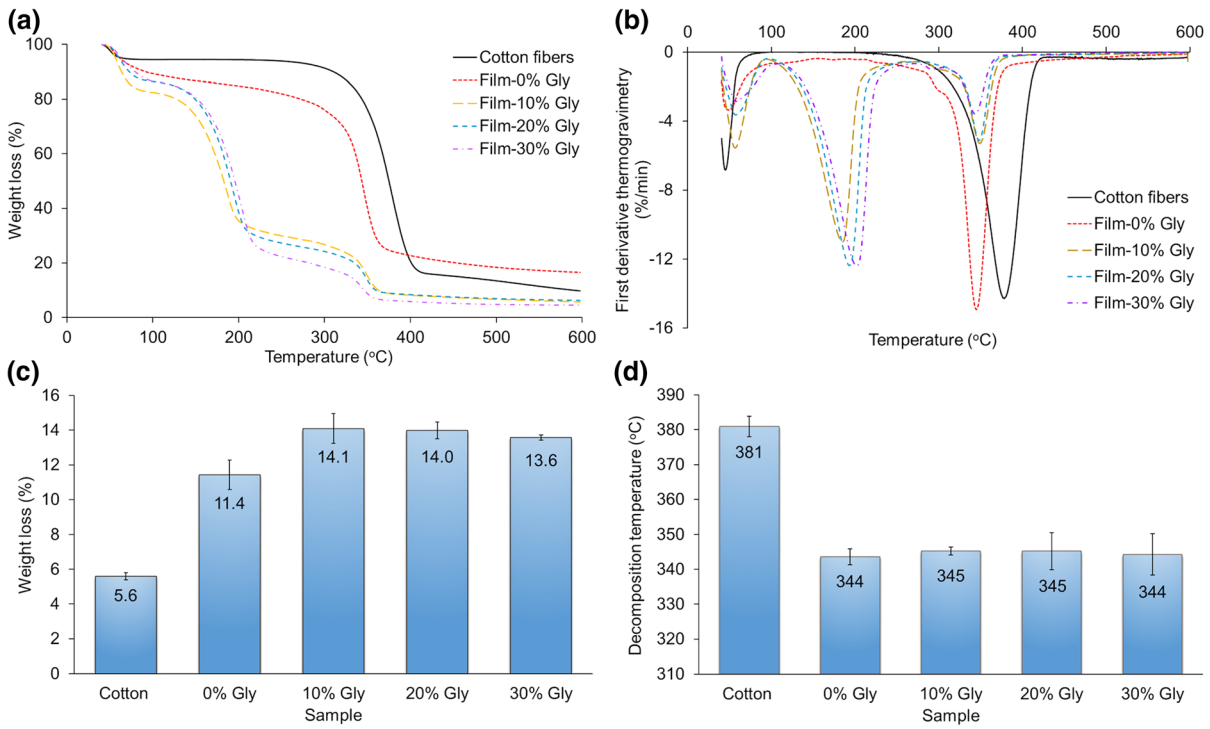

Fig. 5 Thermogravimetric analysis (TGA) of cotton fibers and regenerated cellulose films treated with different concentrations of glycerol: **a** TGA thermograms, **b** first derivative thermogravimetry, **c** percent weight loss due to removal of adsorbed water, and **d** peak decomposition temperatures of cellulose

lower decomposition temperatures than cotton fibers (~ 345 °C) ($p \leq 0.05$). This could be associated with the low crystallinity of cellulose films. Statistical analysis did not reveal a significant effect of glycerol concentration on the thermal decomposition of cellulose films. TGA thermograms of cellulose films prepared from low-quality cotton fibers appear identical to those prepared from pretreated MCC (Ma et al. 2011) and from wood and bamboo pulps (Wang et al. 2013). The hot-pressed cotton cellulose films showed comparable decomposition temperatures to those films prepared by hot-pressing wood and bamboo pulp hydrogels (Wang et al. 2013) and significantly higher degradation temperatures compared to the degradation temperatures of MCC composite films (294–304 °C) (Ma et al. 2011). High temperature tolerance is very important in the field of plastics and for different industrial applications.

Deformation recovery analysis

Figure 6 shows the deformation recovery angles (DRAs) of cellulose films plasticized with different concentrations of cellulose. The DRA of nonplasticized cellulose film is approximately 18°, and it is significantly increased due to plasticization ($p \leq 0.05$, $n = 72$). Recovery from deformation was significantly increased as the glycerol concentration increased up to 30%. Further increase in glycerol concentration did not significantly increase the DRA but affected the integrity of films and made films sticky with poor deformation recovery. Plasticizers create intermolecular hydrogen bonds with cellulose (Xiao et al. 2003), and the inter- and intramolecular hydrogen bonds of cellulose molecules become weaker at high concentrations of plasticizer (Hosokawa et al. 1990; Park et al. 1993; Xiao et al. 2003; Hongphruk and Aht-Ong 2010). The weaker polymer–polymer interaction and/or stickiness could impact the recovery from the deformation of cellulose films treated with > 30% glycerol. Therefore, 30% glycerol was selected as the optimal concentration of glycerol to produce flexible cellulose films from cotton fibers.

Weight change and moisture content analysis

Cellulose itself is a hydrophilic polymer, but the incorporation of glycerol drastically increased the hydrophilicity of cellulose films. Therefore, during water adsorption experiment conducted in a relatively humid environment of 65 ± 2% humidity, plasticized cellulose films rapidly absorbed moisture from the environment compared to nonplasticized films (Fig. 7). After 24 h, glycerol-treated films showed approximately 40% weight gain, whereas nonplasticized films showed only ~ 12% weight gain. Therefore, it is highly desirable to impart hydrophobic characteristics to films to prevent adverse effects of water adsorption in humid environments.

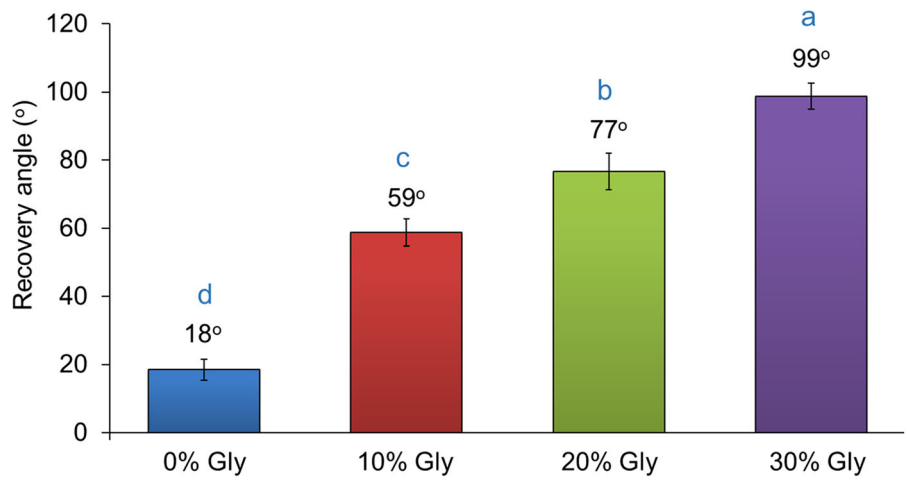

Fig. 6 Deformation recovery angle of cellulose films treated with different concentrations of glycerol. According to the Newman-Keuls test, values not followed by the same letter are significantly different with $\alpha = 5\%$ ($n = 72$)

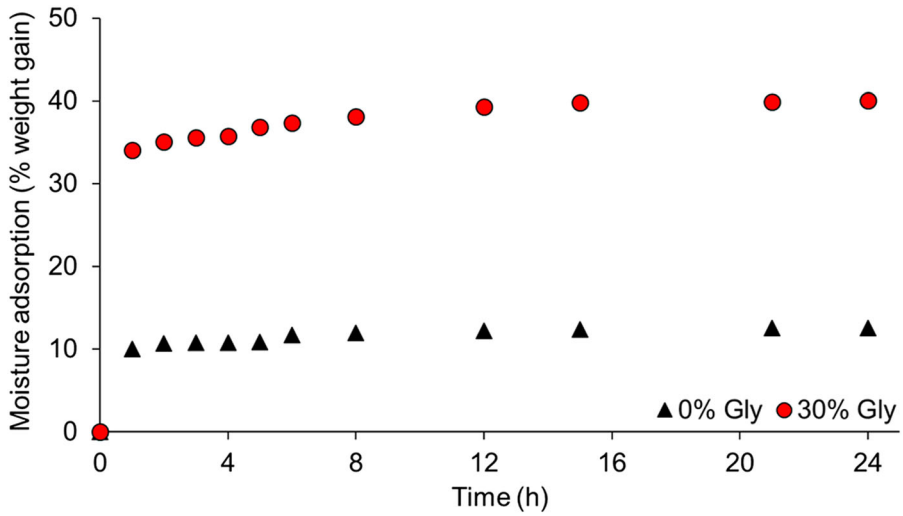

Fig. 7 Moisture absorption of cellulose films in a humid environment (65 ± 2% relative humidity). Nonplasticized cellulose film (0% Gly) and plasticized cellulose film (30% Gly)

Dynamic contact angle analysis

Figure 8 shows the dynamic contact angles of nonplasticized and plasticized cellulose films grafted with different concentrations of oleic acid. Water droplets placed on nonplasticized cellulose film showed an approximately 80° contact angle (Fig. 8a). Grafting with oleic acid did not change the surface hydrophobicity of nonplasticized films (Fig. 8c, e). In contrast, water droplets quickly spread on the surface of plasticized cellulose films due to the increased hydrophilicity associated with glycerol treatment. As shown in Fig. 8b, the initial contact angle of the water droplet on the plasticized film was ∼ 30°, and it immediately dropped within a few seconds. Therefore, surface modification with a hydrophobic agent is desirable to overcome the surface hydrophilicity created by glycerol treatment while preserving the flexibility of films. Surface grafting with oleic acid at concentrations ≤ 0.4 mol/L seemed to minimize the spread of water droplets and increase dynamic contact angles. A higher concentration of oleic acid (> 0.4 mol/l) did not increase water contact angles. Figure 8f shows the change in water droplets on plasticized cellulose films grafted with 0, 0.4, and 1 mol/L oleic acid. A high concentration of oleic acid resulted in the formation of homopolymers, and the second plasma treatment led to the formation of COOH functional groups, which increased the surface hydrophilicity. Therefore, the optimal oleic acid concentration for surface grafting of plasticized cellulose films was 0.4 mol/L. Using this concentration, highly flexible plasticized cellulose films (contact angle ∼ 5°) can achieve reasonable surface hydrophobicity (contact angle ∼ 80°). This contact angle is comparable with that of nonplasticized cellulose film and therefore suggests that surface grafting with 0.4 mol/L oleic acid can overcome the hydrophilicity introduced by glycerol.

Tensile testing

Polymer materials undergo different rates and types of deformation when a stress is applied. This behavior is extremely important for industrial applications of these polymer materials. In the current study, a large number of cellulose films were prepared to determine their behavior under applied stress. Dumbbell-shaped test specimens were prepared using an ASTM D638-14 type IV cutting die and a manual clicker press to minimize inconsistencies introduced during specimen cutting (see supplementary materials—Fig. S5). Figure 9 shows representative stress *vs.* strain curves of nonplasticized and plasticized cellulose films. Table 1 shows the tensile strength and elongation at break, the required energy to break, and Young's modulus of the test specimens and their standard deviations. The results indicate that the two types of cellulose films show major differences in their stress *vs.* strain curves. Nonplasticized films display significantly higher

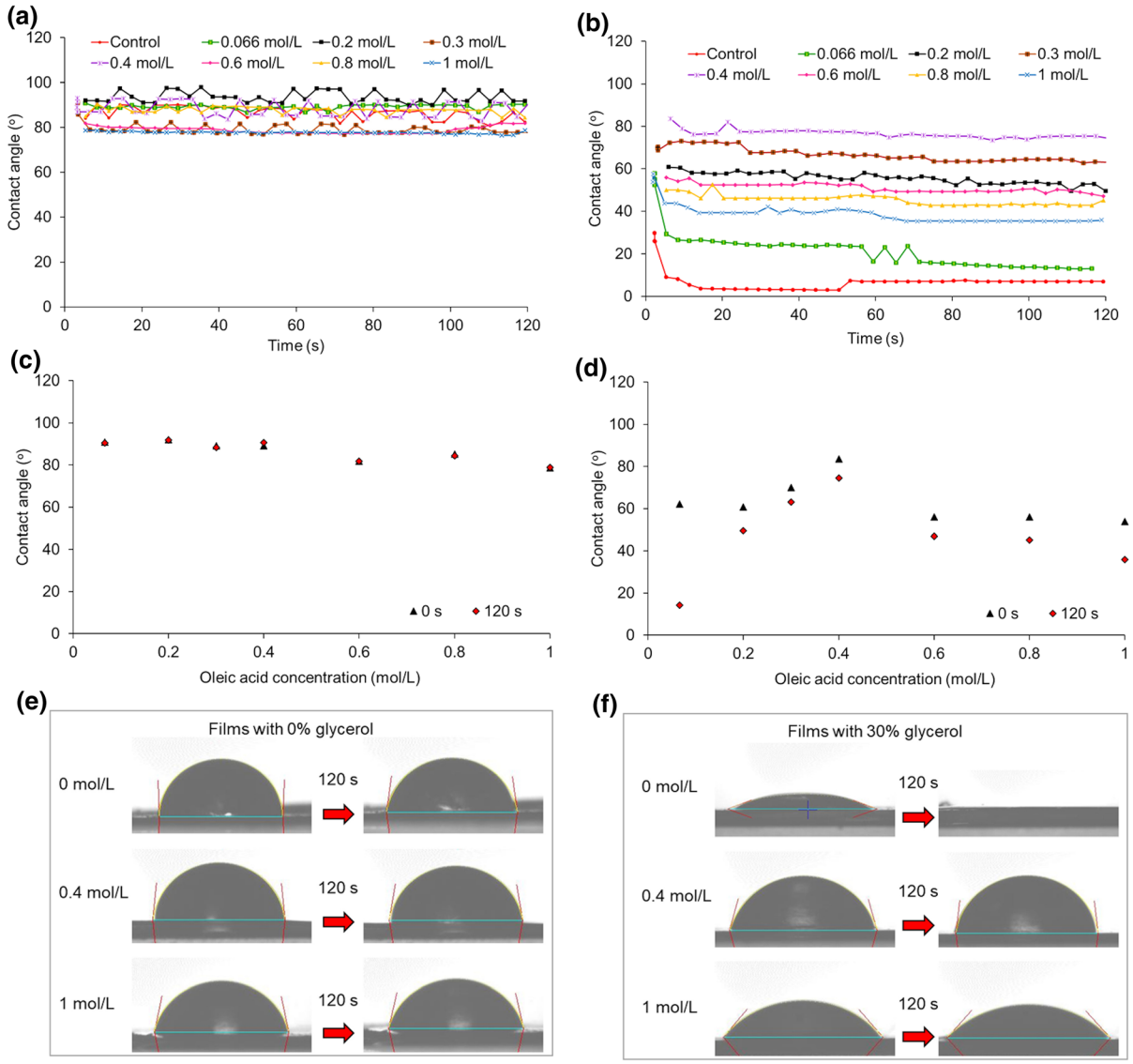

Fig. 8 The effect of oleic acid grafting on the water contact angle of nonplasticized and plasticized cellulose films. Changes in the water contact angle of films grafted with different concentrations of oleic acid within 120 s: **a** nonplasticized and **b** plasticized cellulose film; initial and final water contact angles of cellulose films treated with different concentrations of oleic acid **c** nonplasticized and **d** plasticized cellulose film; and visual changes in water droplets deposited on cellulose films grafted with 0, 0.4, and 1 mol/L oleic acid **e** nonplasticized and **f** plasticized cellulose film

tensile strength (i.e., stress at break) (average = 45–48 kPa) compared to plasticized cellulose films (average 20–23 kPa). In contrast, nonplasticized cellulose films exhibit significantly lower elongation at break (average = 28–38%) compared to plasticized cellulose films (average = 69–77%). Compared to starch-based films, these films show moderate tensile strength and excellent elongation. Sultan and Johari reported that the banana peel films with 4% corn starch had an average tensile strength of 34.7 Pa (Sultan and Johari 2017). Jiménez et al. and Oluwasina et al. reported that plasticized starch films had a higher tensile strength (9.2 MPa, 1.14 MPa), but poor elongation at break (8%, 0.22%) compared to these cellulose films (Jiménez et al. 2012; Oluwasina et al. 2019). Abral et al. reported that tapioca starch bioplastic films had a higher tensile strength

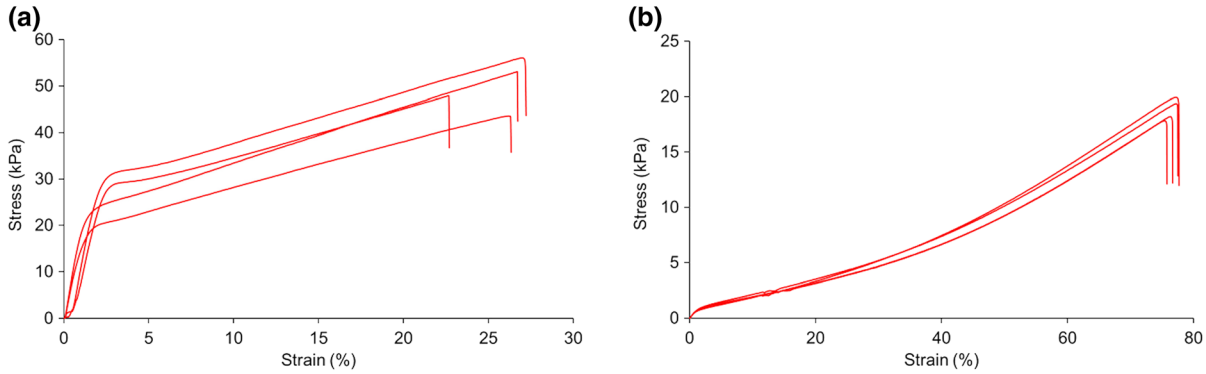

Fig. 9 Stress vs. strain curves of cellulose films. **a** Nonplasticized cellulose films and **b** plasticized cellulose films

Table 1 Tensile strength at break, strain at break, work to break, and Young's modulus of cellulose films

	Replication	Strain at break (%)	Stress at break (kPa)	Work to break (N.mm)	Young's modulus (kPa)
Nonplasticized films	1	38 ± 8	45.9 ± 13.4	1441 ± 480	2317.5 ± 380
	2	28 ± 4	47.2 ± 7.6	1118 ± 160	1490.6 ± 470
	3	35 ± 5	48.5 ± 6.9	1473 ± 371	1403.0 ± 130
	4	31 ± 12	48.1 ± 1.6	1319 ± 500	1520 ± 430
Plasticized films	1	70 ± 10	22.9 ± 4.7	839 ± 150	89.5 ± 34.3
	2	69 ± 9	21.6 ± 2.8	812 ± 160	80.2 ± 17.0
	3	77 ± 16	23.2 ± 1.7	988 ± 220	79.8 ± 15.6
	4	69 ± 8	20.1 ± 3.1	788 ± 160	85.4 ± 22.2

(∼ 1 MPa) and comparable elongation at break (∼ 77%) (Abral et al. 2018).

The toughness of the material is defined as the energy required to break, which is calculated using the area under the load vs. displacement curve. A tough material will not necessarily be the strongest material. A material with lower tensile strength and very high elongation can absorb a significant amount of energy before it reaches the breaking point. In this study, the average area under the stress *vs.* strain curves of nonplasticized and plasticized cellulose films ranged between approximately 1120–1470 and 790–990 N. mm, respectively. Given the variability in each set of samples, both types of cellulose films prepared from low-quality cotton fibers required a comparable amount of energy to break. Nonplasticized cellulose films have a significantly higher Young's modulus (average = 1400–2300 kPa) than plasticized films (average = 80–90 kPa). This means that for the same strain, significantly greater stress is needed for nonplasticized cellulose films compared to that needed for plasticized films. Statistical analysis showed no significant difference in tensile characteristics of cellulose films from different batches ($p \leq 0.05$). The variability within each replication could be associated with irregularities in gelation or inconsistencies introduced during hot pressing.

Conclusions

In this study, highly transparent bioplastic films were prepared from low-quality unmarketable cotton fiber by means of dissolution, casting, regeneration, plasticization, and hot-pressing. It was found that plasticization and hot-pressing play a key role in producing homogeneous cellulose films. Nonplasticized cellulose films were very strong and transparent but were stiffer and less stretchable. Plasticization with glycerol improved the homogeneity, flexibility, stretchability,

and deformation recovery of films. Physical and chemical characterizations indicated that films prepared from cotton fiber were more amorphous with lower crystallinity compared to raw cotton cellulose. The peak decomposition temperatures of cellulose films were observed at approximately 345 °C, and glycerol plasticization did not affect their thermal stability. According to our results, the best deformation recovery was achieved when films were plasticized with 30% glycerol, and further increase in the glycerol concentration produced fragile and sticky films. Glycerol plasticization increased the hydrophilicity of cellulose films. Plasma-induced grafting of oleic acid (concentration = 0.4 mol/L) imparted hydrophobicity to the surface of the films. According to physiochemical and mechanical evaluations of cellulose films made from low-quality cotton fibers, both nonplasticized and plasticized films (with 30% glycerol) are suitable for different industrial applications. Soil burial studies are ongoing to determine the biodegradation behavior of cellulose films under controlled moisture conditions.

Acknowledgments This project was funded by Cotton Incorporated and Texas State Support committee (project numbers: 20-679 and 17-512TX).

References

Abidi N, Cabrales L, Haigler CH (2014) Changes in the cell wall and cellulose content of developing cotton fibers investigated by FTIR spectroscopy. Carbohydr Polym 100:9–16. https://doi.org/10.1016/j.carbpol.2013.01.074

Abidi N, Cabrales L, Hequet E (2010a) Fourier transform infrared spectroscopic approach to the study of the secondary cell wall development in cotton fiber. Cellulose 17:309–320. https://doi.org/10.1007/s10570-009-9366-1

Abidi N, Hequet E, Cabrales L (2010b) Changes in sugar composition and cellulose content during the secondary cell wall biogenesis in cotton fibers. Cellulose 17:153–160. https://doi.org/10.1007/s10570-009-9364-3

Abidi N, Hequet E, Cabrales L et al (2008) Evaluating cell wall structure and composition of developing cotton fibers using Fourier transform infrared spectroscopy and thermogravimetric analysis. J Appl Polym Sci 107:476–486. https://doi.org/10.1002/app.27100

Abidi N, Hequet E, Tarimala S (2007) Functionalization of cotton fabric with vinyltrimethoxysilane. Text Res J 77:668–674. https://doi.org/10.1177/0040517507080621

Abral H, Dalimunthe MH, Hartono J et al (2018) Characterization of tapioca starch biopolymer composites reinforced with micro scale water hyacinth fibers. Starch/Staerke 70:1700287. https://doi.org/10.1002/star.201700287

Acharya S, Hu Y, Moussa H, Abidi N (2017) Preparation and characterization of transparent cellulose films using an improved cellulose dissolution process. J Appl Polym Sci 134:1–12. https://doi.org/10.1002/app.44871

Acharya S, Sultana SR, Parajuli P, Abidi N (2019) Cellulose nanocrystals – sources, preparation, and applications: research advances. In: Croteau O (ed) Cellulose nanocrystals: advances in research and applications, 1st edn. Nova Science Pub Inc, NewYok

ASTM-D638–14 (2015) Standard test method for tensile properties of plastics. ASTM Int 1–15

Brennecke D, Ferreira EC, Costa TMM et al (2015) Ingested microplastics (>100 μm) are translocated to organs of the tropical fiddler crab Uca rapax. Mar Pollut Bull 96:491–495. https://doi.org/10.1016/j.marpolbul.2015.05.001

Brodin M, Vallejos M, Opedal MT et al (2017) Lignocellulosics as sustainable resources for production of bioplastics – a review. J Clean Prod 162:646–664. https://doi.org/10.1016/j.jclepro.2017.05.209

Browne MA, Crump P, Niven SJ et al (2011) Accumulation of microplastic on shorelines woldwide: sources and sinks. Environ Sci Technol 45:9175–9179. https://doi.org/10.1021/es201811s

Cabrales L, Abidi N (2012) Microwave plasma induced grafting of oleic acid on cotton fabric surfaces. Appl Surf Sci 258:4636–4641. https://doi.org/10.1016/j.apsusc.2011.12.130

Carrillo F, Colom X, Suñol JJ, Saurina J (2004) Structural FTIR analysis and thermal characterisation of lyocell and viscose-type fibres. Eur Polym J 40:2229–2234. https://doi.org/10.1016/j.eurpolymj.2004.05.003

Ciolacu D, Ciolacu F, Popa VI (2011) Amorphous cellulose–structure and characterization. Cellul Chem Technol 45:13–21

Dissanayake N, Thalangamaarachchige VD, Thakurathi M et al (2019) Dissolution of cotton cellulose in 1:1 mixtures of 1-butyl-3-methylimidazolium methylphosphonate and 1-alkylimidazole co-solvents. Carbohydr Polym 221:63–72. https://doi.org/10.1016/j.carbpol.2019.05.071

Edgar KJ, Buchanan CM, Debenham JS et al (2001) Advances in cellulose ester performance and application. Prog Polym Sci 26:1605–1688. https://doi.org/10.1016/S0079-6700(01)00027-2

El Seoud OA, Marson GA, Ciacco GT, Frollini E (2000) An efficient, one-pot acylation of cellulose under homogeneous reaction conditions. Macromol Chem Phys 201:882–889. https://doi.org/10.1002/(sici)1521-3935(20000501)201:8%3c882::aid-macp882%3e3.3.co;2-9

Fink H-P, Weigel P, Purz H, Ganster J (2001) Structure formation of regenerated cellulose materials from NMMO-solutions. Prog Polym Sci 26:1473–1524. https://doi.org/10.1016/S0079-6700(01)00025-9

French AD (2014) Idealized powder diffraction patterns for cellulose polymorphs. Cellulose 21:885–896. https://doi.org/10.1007/s10570-013-0030-4

Geyer R, Jambeck JR, Law KL (2017) Production, use, and fate of all plastics ever made. Sci Adv 3:e1700782. https://doi.org/10.1126/sciadv.1700782

Gwon JG, Lee SY, Doh GH, Kim JH (2010) Characterization of chemically modified wood fibers using FTIR spectroscopy for biocomposites. J Appl Poly Sci 116:3212–3219

Hongphruk P, Aht-Ong D (2010) Effect of plasticizers on the mechanical properties of cellulose laurate films. Adv Mater Res 93–94:117–120. https://doi.org/10.4028/www.scientific.net/AMR.93-94.117

Hosokawa J, Nishiyama M, Yoshihara K, Kubo T (1990) Biodegradable film derived from chitosan and homogenized cellulose. Ind Eng Chem Res 29:800–805. https://doi.org/10.1021/ie00101a015

Hsieh YL (2007) Chemical structure and properties of cotton. In: Gordon S, Hsieh YL (eds) cotton, 1st edn. Woodhead Publishing, Cambridge

Hu Y, Abidi N (2016) Distinct chiral nematic self-assembling behavior caused by different size-unified cellulose nanocrystals via a multistage separation. Langmuir 32:9863–9872. https://doi.org/10.1021/acs.langmuir.6b02861

Hurtubise FG, Krassig H (1960) Classification of fine structural characteristics in cellulose by infared spectroscopy. Use of potassium bromide pellet technique. Anal Chem 32:177–181. https://doi.org/10.1021/ac60158a010

Jiménez A, Fabra MJ, Talens P, Chiralt A (2012) Effect of re-crystallization on tensile, optical and water vapour barrier properties of corn starch films containing fatty acids. Food Hydrocoll 26:302–310. https://doi.org/10.1016/j.foodhyd.2011.06.009

Karami A, Golieskardi A, Keong Choo C et al (2017) The presence of microplastics in commercial salts from different countries. Sci Rep 7:1–11. https://doi.org/10.1038/srep46173

Klemm D, Heublein B, Fink H-P, Bohn A (2005) Cellulose: Fascinating biopolymer and sustainable raw material. Angew Chemie Int Ed 44:3358–3393. https://doi.org/10.1002/anie.200460587

Laist DW (1997) Impacts of Marine Debris: Entanglement of Marine Life in Marine Debris Including a Comprehensive List of Species with Entanglement and Ingestion Records. 99–139. https://doi.org/https://doi.org/10.1007/978-1-4613-8486-1_10

Lan W, Liu C-F, Yue F-X et al (2011) Ultrasound-assisted dissolution of cellulose in ionic liquid. Carbohydr Polym 86:672–677. https://doi.org/10.1016/j.carbpol.2011.05.013

Law KL, Thompson RC (2014) Microplastics in the seas. Science 345(80):144–145. https://doi.org/10.1126/science.1254065

Ling SD, Sinclair M, Levi CJ et al (2017) Ubiquity of microplastics in coastal seafloor sediments. Mar Pollut Bull 121:104–110. https://doi.org/10.1016/j.marpolbul.2017.05.038

Liyanage S, Abidi N (2019) Molecular weight and organization of cellulose at different stages of cotton fiber development. Text Res J 89:726–738. https://doi.org/10.1177/0040517517753642

Lu Y, Weng L, Cao X (2005) Biocomposites of plasticized starch reinforced with cellulose crystallites from cottonseed linter. Macromol Biosci 5:1101–1107. https://doi.org/10.1002/mabi.200500094

Luo X, Zhang L (2013) New solvents and functional materials prepared from cellulose solutions in alkali/urea aqueous system. Food Res Int 52:387–400. https://doi.org/10.1016/j.foodres.2010.05.016

Ma H, Zhou B, Li HS et al (2011) Green composite films composed of nanocrystalline cellulose and a cellulose matrix regenerated from functionalized ionic liquid solution. Carbohydr Polym 84:383–389. https://doi.org/10.1016/j.carbpol.2010.11.050

Mathalon A, Hill P (2014) Microplastic fibers in the intertidal ecosystem surrounding Halifax Harbor, Nova Scotia. Mar Pollut Bull 81:69–79. https://doi.org/10.1016/j.marpolbul.2014.02.018

McCormick CL, Callais PA, Hutchinson BH (1985) Solution studies of cellulose in lithium chloride and N, N-dimethylacetamide. Macromolecules 18:2394–2401. https://doi.org/10.1021/ma00154a010

Mekonnen T, Mussone P, Khalil H, Bressler D (2013) Progress in bio-based plastics and plasticizing modifications. J Mater Chem A 1:13379–13398. https://doi.org/10.1039/c3ta12555f

Moon RJ, Martini A, Nairn J et al (2011) Cellulose nanomaterials review: structure, properties and nanocomposites. Chem Soc Rev 40:3941–3994. https://doi.org/10.1039/c0cs00108b

Nelson ML, Mares T (1965) Accessibility and lateral order distribution of the cellulose in the developing cotton fiber1. Text Res J 35:592–603. https://doi.org/10.1177/004051756503500703

Oh SY, Dong IY, Shin Y et al (2005) Crystalline structure analysis of cellulose treated with sodium hydroxide and carbon dioxide by means of X-ray diffraction and FTIR spectroscopy. Carbohydr Res 340:2376–2391. https://doi.org/10.1016/j.carres.2005.08.007

Olivier-Bourbigou H, Magna L, Morvan D (2010) Ionic liquids and catalysis: recent progress from knowledge to applications. Appl Catal A Gen 373:1–56. https://doi.org/10.1016/j.apcata.2009.10.008

Oluwasina OO, Olaleye FK, Olusegun SJ et al (2019) Influence of oxidized starch on physicomechanical, thermal properties, and atomic force micrographs of cassava starch bioplastic film. Int J Biol Macromol 135:282–293. https://doi.org/10.1016/j.ijbiomac.2019.05.150

Park HJ, Weller CL, Vergano PJ, Testin RF (1993) Permeability and mechanical properties of cellulose-based edible films.

J Food Sci 58:1361–1364. https://doi.org/10.1111/j.1365-2621.1993.tb06183.x

Park HM, Misra M, Drzal LT, Mohanty AK (2004) "Green" nanocomposites from cellulose acetate bioplastic and clay: effect of eco-friendly triethyl citrate plasticizer. Biomacromol 5:2281–2288. https://doi.org/10.1021/bm049690f

Qi H, Yang Q, Zhang L et al (2011) The dissolution of cellulose in NaOH-based aqueous system by two-step process. Cellulose 18:237–245. https://doi.org/10.1007/s10570-010-9477-8

Rogers RD, Seddon KR (2003) Chemistry: ionic liquids-solvents of the future? Science 302:792–793. https://doi.org/10.1126/science.1090313

Rosenau T, Potthast A, Adorjan I et al (2002) Cellulose solutions in N-methylmorpholine-N-oxide (NMMO) - degradation processes and stabilizers. Cellulose 9:283–291. https://doi.org/10.1023/A:1021127423041

Sayyed AJ, Deshmukh NA, Pinjari DV (2019) A critical review of manufacturing processes used in regenerated cellulosic fibres: viscose, cellulose acetate, cuprammonium, LiCl/DMAc, ionic liquids, and NMMO based lyocell. Cellulose 26:2913–2940. https://doi.org/10.1007/s10570-019-02318-y

Sen S, Martin JD, Argyropoulos DS (2013) Review of cellulose non-derivatizing solvent interactions with emphasis on activity in inorganic molten salt hydrates. ACS Sustain Chem Eng 1:858–870. https://doi.org/10.1021/sc400085a

Sultan NFK, Johari WLW (2017) Bioremediation science and technology the development of banana peel / corn starch bioplastic film: a preliminary study. Bioremediation Sci Technol Res 5:12–17

Suyatma NE, Tighzert L, Copinet A, Coma V (2005) Effects of hydrophilic plasticizers on mechanical thermal and surface properties of chitosan films. J Agric Food Chem 53:3950–3957. https://doi.org/10.1021/jf048790+

Swatloski RP, Spear SK, Holbrey JD, Rogers RD (2002) Dissolution of cellose with ionic liquids. J Am Chem Soc 124:4974–4975. https://doi.org/10.1021/ja025790m

Teuten EL, Saquing JM, Knappe DRU et al (2009) Transport and release of chemicals from plastics to the environment and to wildlife. Philos Trans R Soc B Biol Sci 364:2027–2045. https://doi.org/10.1098/rstb.2008.0284

Tourinho PS, Ivar do Sul JA, Fillmann G, (2010) Is marine debris ingestion still a problem for the coastal marine biota of southern Brazil? Mar Pollut Bull 60:396–401. https://doi.org/10.1016/j.marpolbul.2009.10.013

Vethaak AD, Leslie HA (2016) Plastic debris is a human health issue. Environ Sci Technol 50:6825–6826. https://doi.org/10.1021/acs.est.6b02569

Wang H, Gurau G, Rogers RD (2012) Ionic liquid processing of cellulose. Chem Soc Rev 41:1519–1537. https://doi.org/10.1039/c2cs15311d

Wang Q, Cai J, Zhang L et al (2013) A bioplastic with high strength constructed from a cellulose hydrogel by changing the aggregated structure. J Mater Chem A 1:6678–6686. https://doi.org/10.1039/c3ta11130j

Xiao C, Zhang Z, Zhang J et al (2003) Properties of regenerated cellulose films plasticized with α-monoglycerides. J Appl Polym Sci 89:3500–3505. https://doi.org/10.1002/app.12509

Zhang L, Mao Y, Zhou J, Cai J (2005) Effects of coagulation conditions on the properties of regenerated cellulose films prepared in NaOH/urea aqueous solution. Ind Eng Chem Res 44:522–529. https://doi.org/10.1021/ie0491802

Zhang L, Ruan D, Gao S (2002) Dissolution and regeneration of cellulose in NaOH/thiourea aqueous solution. J Polym Sci Part B Polym Phys 40:1521–1529. https://doi.org/10.1002/polb.10215

Zhang L, Ruan D, Zhou J (2001) Structure and properties of regenerated cellulose films prepared from cotton linters in NaOH/urea aqueous solution. Ind Eng Chem Res 40:5923–5928. https://doi.org/10.1021/ie0010417

Zhou J, Zhang L (2000) Solubility of cellulose in NaOH urea. Polym J 32:866–870

Zhou J, Zhang L, Shu H, Chen F (2002) Regenerated cellulose films from NaOH/urea aqueous solution by coagulating with sulfuric acid. J Macromol Sci Part B 41:1–15. https://doi.org/10.1081/MB-120002342